# Fluctuating temperature measurements on a cylinder in a cross-flow using fiber-optic Bragg grating sensors

by

Z. J. Wang, X. W. Wang, Y. Zhou* and W. O. Wong

Department of Mechanical Engineering

The Hong Kong Polytechnic University

Hung Hom, Kowloon, Hong Kong

*E-Mail: mmyzhou@polyu.edu.hk

**ABSTRACT**

A fiber-optic Bragg grating (FBG) sensor is proposed to measure the local static temperature $\overline{q_s}$ and the fluctuating temperature $q_s$ on the surface of a heated circular cylinder subjected to a cross-flow. In order to validate the new technique, a type-*K* thermocouple and a single hot-wire are used to measure $\overline{q_s}$ and the near-wake streamwise fluctuating velocity *u*, respectively. The FBG sensor measurement of $\overline{q_s}$ agrees well with that simultaneously obtained by the thermocouple. The $q_s$-spectrum exhibits a prominent peak at the vortex shedding frequency, $f_s^* = \frac{f_s d}{U_\infty} \approx 0.2$ ($U_\infty$ is the free-stream velocity and *d* is the cylinder diameter), consistent with the *u*-spectrum. In fact, the $q_s$ and *u* signals are almost perfectly correlated at $f_s^*$. Furthermore, the measured $\overline{q_s}$ and root mean square value of $q_s$ are agreeable with previously reported Nusselt number data. These results demonstrate that the FBG sensor can be used to measure reliably both static and fluctuating temperatures. It is expected that the FBG sensor, because of its uniqueness in many aspects and being at an affordable cost, has an excellent prospect in temperature measurements.

## 1. INTRODUCTION

The study of the heat transfer characteristics of a heated circular cylinder in a cross-flow is of practical significance. As the Reynolds number, *Re*, exceeds a critical value, the boundary layer separates from the cylinder in a flip-flop manner. The separation point oscillates on the cylinder surface with an excursion of about 10° (Achenbach 1968; Dwyer and Mccroskey 1973; Higuchi *et al*. 1989) and its mean location is dependent on *Re* (Chen 1987). Naturally, the surface temperature fluctuates and the circumferential distribution of the static temperature is non-uniform. Local heat transfer from the cylinder to fluid varies azimuthally (Giedt 1949; Krall and Eckert 1973; Scholten and Murray 1998).

Experimental investigations of the heat transfer problem around a cylinder have been concentrated mainly on the measurement of the overall and local heat transfer coefficients, which were usually achieved by measuring the local heat flux and simultaneously the difference between local static surface temperature and bulk flow temperature (e. g. Perking and Leppert 1964; Zukauskas and Ziugzda 1985). Boulos and Pei (1973) provided an excellent compendium of experimental and theoretical works on this topic. The data of the local fluctuating surface temperature is however scarce in spite of its significance in understanding the physics of heat transfer.

A number of well-established techniques are available for temperature measurements (Valvano 1992). Morris (1993) divided these techniques into eight categories based on their operating principle, i.e. thermal expansion method, thermocouples, resistive sensors, quartz thermometers, radiation thermometers, thermograph (thermal imaging), acoustic thermometers and fiber optic temperature sensors. Most of these techniques are suitable either for a particular situation or for the measurement of the static temperature. For example, thermograph provides the static temperature distribution over a surface. Radiation thermometers are non-invasive, though largely suitable for a high temperature situation. Acoustic thermometers cater for needs to measure cryogenic temperature (Morris 1993). Fluctuating temperatures may be measured using thermocouples, resistive sensors (Morrison 1984; Michalski *et al*. 1991; Morris 1993). Thermocouples suffer from a poor dynamic response and consequently are generally used measure the static temperature or fluctuating temperature of a low frequency (Valvano 1992). In the presence of a flow, this technique may be intrusive to the flow. Resistive sensors, such as fine wires used in the gas flow or thin metal films for solid surfaces, have good dynamic responses. However, this kind of sensors is usually associated with a bridge circuit, which may alter the temperature field under investigation (Marton and Marton 1981). Furthermore, both thermocouples and resistive sensors are prone to corruption by a neighbouring electromagnetic field.

The fiber optic technique is relatively new for temperature sensors (Michalski *et al*. 1991; Morris 1993). Gottlieb and Brandt (1979) described the temperature-induced change of the refractive index of an optical fiber for measuring average temperature along its length. A typical application of fiber optic temperature sensors is to monitor, or measure the average temperature or temperature distribution of large surfaces or long objects (Sandberg and Haile 1987; Grattan 1987; Michalski *et al*. 1991).

In the present study, it is proposed to use an alternative technique, the fiber-optic Bragg grating (FBG) sensor, to measure both static and fluctuating temperatures on the surface of a heated circular cylinder in a cross-flow. Hill *et al*. (1978) first reported this sensor. A fiber Bragg grating (FBG) is produced by varying the refractive index along an optical fiber. Since then, the FBG sensor has attracted considerable interest in various fields of engineering, including telecommunications, instrumentation and the measurements of strain, temperature and hydrostatic pressure (Morey *et al*. 1989). The FBG sensor has many unique features. For example, its diameter could be as small as 80μm. Therefore, its attachment to the structure would not seriously compromise the flow around the structure (Zhou *et al*. 1999; Jin *et al*. 2000). Its dynamic response is excellent. Furthermore, it is immune to corruption by neighbouring electromagnetic field and also causes no disturbance to the temperature field. In view of these advantages, the technique is most attractive for temperature measurements.

## 2. FBG SENSOR SYSTEM

The FBG sensing system was built in-house (Ho *et al*. 2002). It consists of a tunable narrow-band light source, a fiber coupler, a sensing FBG, a reference FBG, a photo-detector, a low pass electrical filter, a high pass electrical filter and the data acquisition & signal processing system (Figure 1). The tunable narrow-band light source is a combination of a broadband light source and a tunable optical filter (TOF). The reference FBG is isolated from the environmental effect and used as a reference to minimize the effect of drift and non-

repeatability of the TOF. Signal from the photo-detector is processed to give two outputs, one ($V_{DC}$) for static temperature measurement, the other ($V_{AC}$) for dynamic measurement.

An FBG is formed inside the core of an optical fiber by introducing a periodic change in the refractive index along the fiber (Figure 1). Assuming the input signal is broadband light incident on the grating, a narrow band signal is reflected back at the Bragg resonance wavelength $l_B = 2n\Lambda$ (Kersey *et al*. 1997), where ? is the grating pitch and *n* the averaged fiber refractive index. When an optical fiber built with an FBG sensor is bounded on the surface of the structure along the cylinder span, the fiber and the FBG sensor will follow the surface temperature of the cylinder. Any perturbation, say due to applied temperature variation, *q*, of the grating results in a variation in ? and *n*, and therefore a shift $\Delta l_B$ in $l_B$. The value of $\Delta l_B$ is related to *q* by $\Delta l_B = Kq$, where *K* is a scale factor and can be determined by a calibration process. Using a wavelength detection device, $\Delta l_B$ can be converted into the variation of light intensity. The intensity variation is subsequently converted into an electric current or voltage through a photo-detector. Therefore, *q* is related to that of the electric signal.

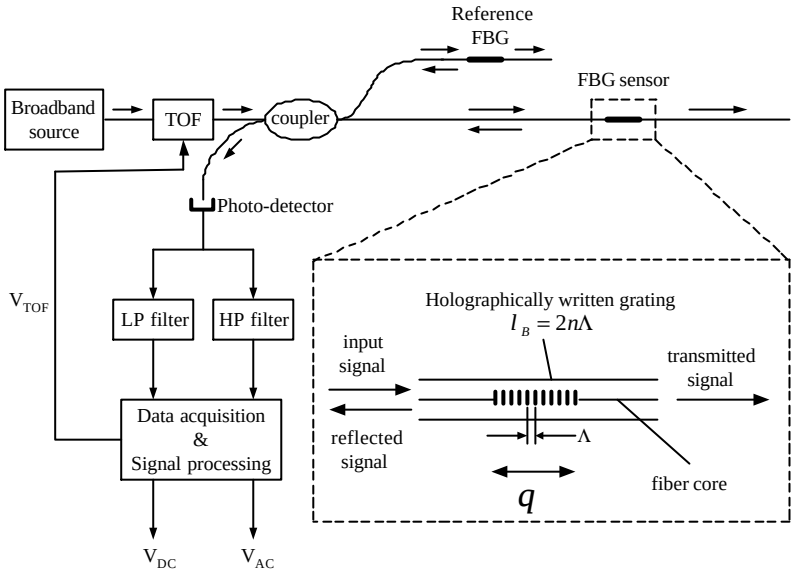


*Figure 1. A schematic of the fiber-optic Bragg grating sensing system (adapted from Kersey et al. 1997; Ho et al. 2002). LP and HP stand for low pass and high pass, respectively.*

The static temperature measurement is carried out by scanning the TOF and recording the TOF control voltages $V_{TOF} = V_r$ and $V_{TOF} = V_s$, which correspond to the center wavelength of the TOF aligned to the Bragg wavelengths of the reference and sensing FBGs, respectively. The Bragg wavelength of the reference grating is kept constant, while the Bragg wavelength of the sensing grating varies with *q*. The differential voltage $V_s$-$V_r$ is proportional to the difference between the two Bragg wavelengths and is therefore to the applied static temperature. The dynamic temperature measurement is performed by the following procedure: after the aforementioned scan is completed, the TOF control voltage $V_{TOF}$ is tuned to and held at a constant value $V_o = V_s + \Delta V_s$, corresponding to a maximum slope point on the reflection spectrum of the sensing FBG. Around this operating point, the sensor response is linear and most sensitive to a small dynamic temperature. Any dynamic temperature applied to the sensing grating is transformed linearly into a light intensity variation that is converted into a time varying voltage ($V_{AC}$) at the photo-detector output. The value of $\Delta V_s$ is determined by the spectral characteristic of the sensing grating. By repeating the scanning-and-holding process, the static and dynamic temperatures can be measured alternatively. The scanning and holding times can be adjusted and should be selected carefully to optimize the measurement performance.

## 3. EXPERIMENTAL DETAILS

Experiments were conducted in a suction-type wind tunnel with a 0.5m long working section (0.35m × 0.35m). A brass circular cylinder of diameter $d$ = 19.0 mm was vertically mounted in the mid-plane of the working section, 20 cm from the exit plane of the contraction. This resulted in a blockage of about 5.4% and an aspect

ratio of 18. The cylinder vibration is negligible because of a very large structural rigidity. The cylinder was electrically heated. The Reynolds number *Re* ($\equiv U_\infty d/n$, where $U_¥$ is the free stream velocity and ν the fluid kinematic viscosity) investigated varied from 7,600 to 35,000. In the free stream, the longitudinal turbulence intensity was about 0.2%.

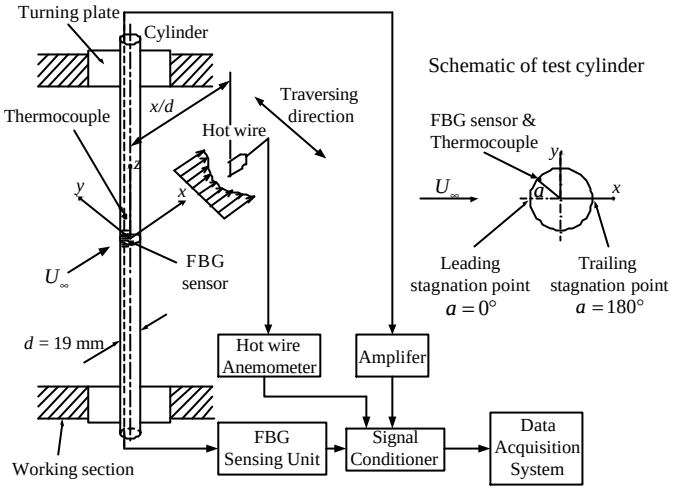


*Figure 2. Experimental arrangement.*

The experimental arrangement is shown schematically in Figure 2. The wake fluctuating velocity *u* was monitored by a single Tungsten hot wire located at *x/d* = 2 and *y/d* = 1.5, where *x* and *y* are the stream-wise and lateral coordinates, respectively, whose origin is chosen at the cylinder center. The hot wire was operated at an overheat ratio of 1.8 with a constant temperature anemometer.

A groove of about 250 μm deep was made along the cylinder span to lay an optical fiber of diameter 250 μm. The fiber, flush with the cylinder surface using heat-conducting silicone, was built with an FBG sensor. The sensor, located at the mid-span of the cylinder, measured the static temperature $\overline{q_s}$ and fluctuating temperature $q_s$ on the cylinder surface. By rotating the cylinder, the circumferential distribution of temperature was measured. Assuming a symmetrical distribution about the *x*-axis, $\overline{q_s}$ and $q_s$ were measured from $a$ = 0° to 180° only, where $a$ = 0° and 180° corresponds to the leading and trailing stagnation points, respectively. In order to validate the FBG sensor measurement, $\overline{q_s}$ was simultaneously measured using a type-*K* thermocouple placed at the same $a$ as the FBG sensor but 0.02 m (≈ 1*d*) away in the spanwise direction. As the boundary layer separates from the cylinder, the vortex cell is characterized by a typical spanwise extent of 1 ~ 3*d* (King 1977; Higuchi *et al*. 1989). Therefore, the static surface temperature captured by the thermocouple should be the same as that by the FBG sensor.

The signals $u, q_s$ and $\overline{q_s}$ were simultaneously measured and amplified and then digitised using a 12bit A/D board and a personal computer at a sampling frequency of 3.5kHz per channel. The duration of each record was 20 seconds. This has been verified to be sufficiently long for the root mean square (rms) value, $q_{s,rms}$, of $q_s$ to reach approximately constant, with a variation smaller than 1.0%.

## 4. STATIC TEMPERATURE

For the purpose of comparison, the measured temperature is normalized by the overall mean surface temperature, $\Theta = \frac{1}{n}\sum_{i=1}^{n}\overline{q_s}(i)$, where $\overline{q_s}(i)$ represents the measured local static surface temperature and $n$ is the total

number of $\overline{q_s}$ measured around the cylinder surface for each *Re*. Figure 3 presents both FBG sensor and thermocouple measurements of $\overline{q_s}/\Theta$ at Re = 7600. The two techniques show a good agreement, thus providing a validation for the FBG sensor measurement.

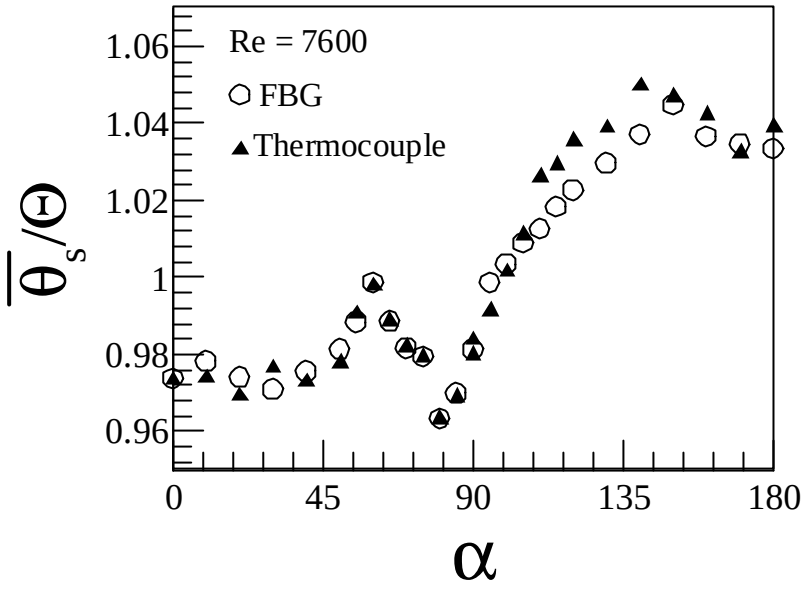


*Figure 3. Circumferential distributions of the local static surface temperature* $\overline{q_s}/\Theta$ *measured using the FBG sensor (?) and a type-K thermocouple (? ). (Re = 7600).*

The circumferential distribution of the heat-transfer coefficient, i.e. the Nusselt number *Nu*, around the cylinder surface has been well documented for different *Re* (e.g. Giedt 1949; Krall and Eckert 1973; Boulos and Pei 1974). The circumferential distribution of $\overline{q_s}/\Theta$ is qualitatively consistent with the reported *Nu* data (e.g. Holman 1997). Before flow separation, as *a* increases, the heat transfer is adversely affected by the growing laminar boundary layer and thus *Nu* gradually decreases. *Nu* reaches the minimum at the point of the boundary layer separation. Correspondingly, $\overline{q_s}/\Theta$ rises from $a$ = 0 up to 60° (Figure 3), which is likely to correspond to the minimum local *Nu* or approximately the flow separation point. Indeed, the extrapolation of Giedt (1949)'s measurement of *Nu* at *Re* larger than in the present investigation indicates that the minimum *Nu* occurs around $a \approx 60°$ for the present *Re*. It is worthwhile pointing out that the separation point oscillates and its excursion is usually within 10°, varying from $a$ = 75° to 85° for Re = $1.06 \times 10^5$ (Dwyer e*t al*. 1973). The mean location of flow separation is dependent upon *Re* (Chen 1987). For example, Higuchi *et al*. (1989) found that the separation point oscillated between 87° and 95° at *Re* = $1.96 \times 10^5$, while Achenbach (1968) reported that boundary layer separation occurred at 78° for Re = $10^5$ and shifted to 94° for Re = $3 \times 10^5$. Again, these experimental data may be extrapolated, suggesting the occurrence of the separation point near $a \approx 60°$. There is a subsequent drop between $a \approx 60°$ and 80° in $\overline{q_s}/\Theta$ due to a corresponding increase in *Nu*. The increased *Nu* results from the turbulent motion in the separated flow, which may perturb the laminar sublayer that is responsible for the main thermal resistance associated with the convective heat transfer (Holman 1997). For $a > 80°$, $\overline{q_s}/\Theta$ climbs steadily probably due to the recirculation effect. Since vortex shedding would produce a strong back-flow over the rear portion of the cylinder (Goldstein 1965), the local heat transfer coefficient increases. Consequently, $\overline{q_s}/\Theta$ decreases slightly near the trailing stagnation point ($a$ = 180°).

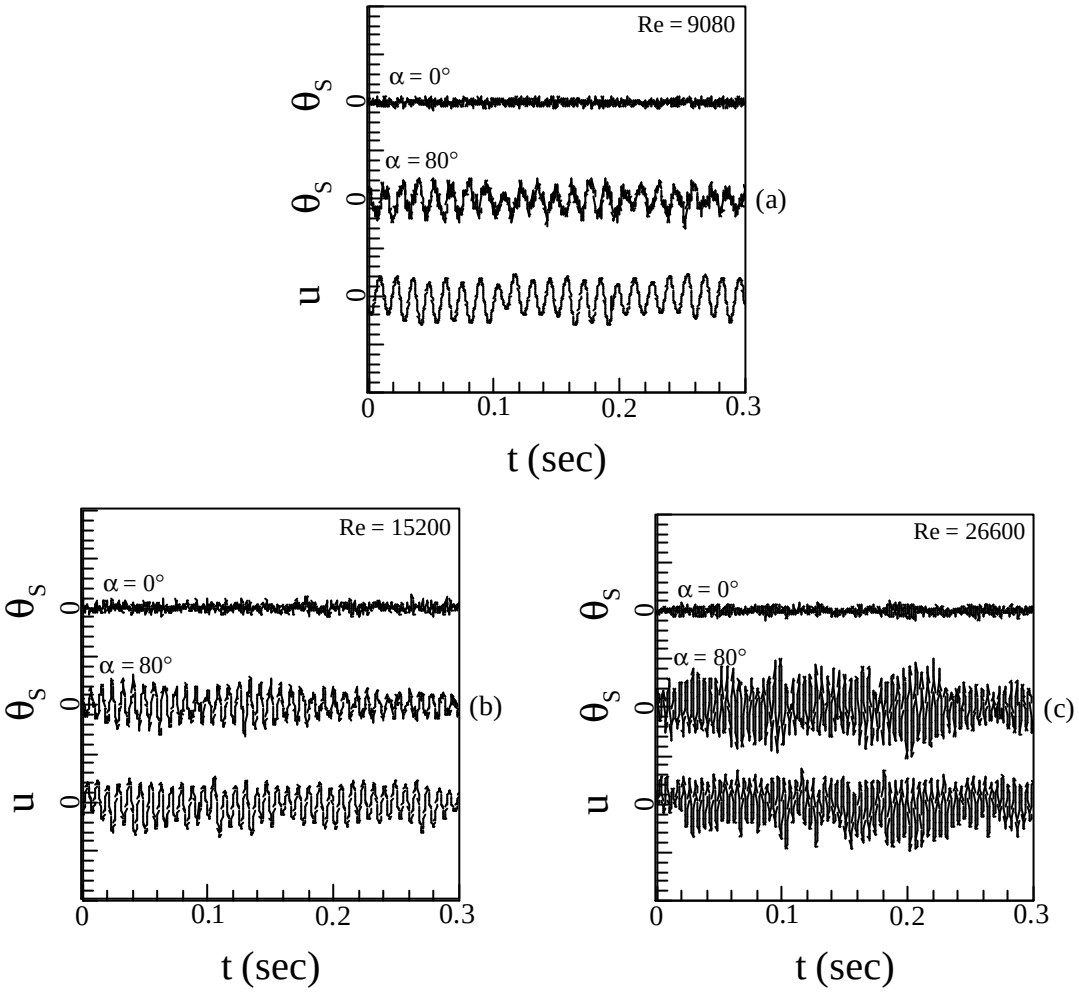


*Figure 4. Time histories of u (the hot wire was located at x/d = 2 and y/d = 1.5) and $q_s$ at $a$ = 0° and 80°. (Time t = 0 is arbitrary). (a) Re = 9080; (b) Re = 15200; (c) Re = 26600.*

## 5. FLUCTUATING TEMPERATURE

### 5.1 Time Series and Their Spectra

Figure 4 shows the time histories of $q_s$ at $a$ = 0° (upper trace) and $a$ = 80° (middle trace), where the minimum $\overline{q_s}/\Theta$ occurs, along with the simultaneously measured *u* (lower trace), for different *Re*. The same scales are used for the signals at different Re to facilitate comparison. For all *Re*, the $q_s$ signal at $a$ = 80° exhibits a quasi-periodic fluctuation, which is also evident in the *u* signal, apparently due to vortex shedding. In general, the maximum amplitude of $q_s$ grows with *Re*. The $q_s$ signal at $a$ = 0° is quite different from that at $a$ = 80°. A pseudo-periodic fluctuation is also evident, but its magnitude is much smaller than at $a$ = 80°. Furthermore, the dominant fluctuation frequency appears higher. The dominant frequencies are better identified in the power spectra, $E_{q_s}$ and $E_u$ (Figure 5), of $q_s$ and *u* (Re = 15200). Both $E_{q_s}$ and $E_u$ display one major peak at $f_s^* = f_s d/U_\infty \approx 0.2$, which is consistent with the vortex shedding frequency of a single cylinder (Schlichting 1979). Another peak in $E_{q_s}$ occurs at $f^* \approx 0.4$, which is probably the second harmonic of $f_s^*$. This peak is more evident at $a$ = 0°, where $q_s$ reflects vortex shedding on both sides. The observation is consistent with Scholten

and Murray (1998)'s report that the time trace of the heat flux signal at the forward stagnation point fluctuated at $2f_s^*$. It is pertinent to comment that $E_{q_s}$ and $E_u$ display identical dominant frequencies at say $f_s^*$. This is confirmed for all Re investigated, suggesting that the FBG sensor has a small thermal inertia and its dynamic response is adequate to resolve the fluctuating temperature on the cylinder surface.

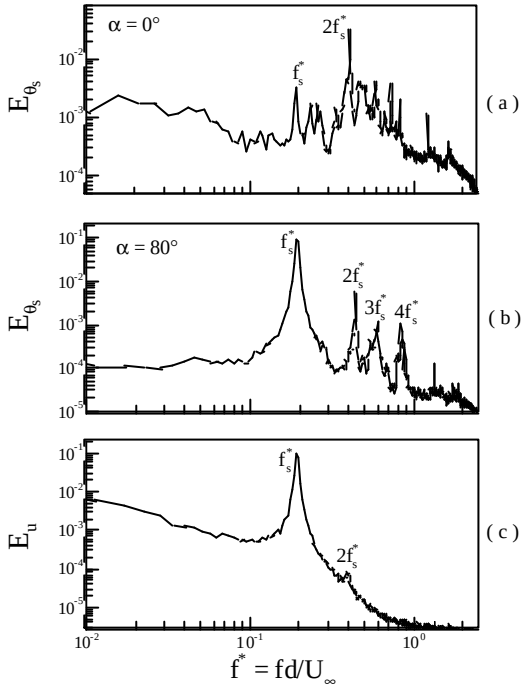


*Figure 5. Power spectrum $E_{q_s}$ of the fluctuating surface temperature $q_s$ and $E_u$ of the streamwise fluctuating velocity u in the wake. Re = 15200. (a) $E_{q_s}$ at a = 0°; (b) $E_{q_a}$ at a = 80°; (c) $E_u$. The hot wire was located at x/d = 2 and y/d = 1.5.*

The test cylinder, fix-supported at both ends, may vibrate due to vortex excitation forces, which produces a structural dynamic strain (e.g. Zhou *et al*. 2001). The strain may reflect on the optic fiber, leading to a shift $\Delta l_B$ in $l_B$ (Zhou *et al*. 1999; Jin *et al*. 2000). Consequently, the measured fluctuating temperature signal might be contaminated. It is therefore important to ensure a negligible contamination in the present investigation. A test was thus conducted at conditions identical to those described for the fluctuating temperature measurements in Section 3, except the cylinder was unheated. Figure 6 presents the $q_s$ signal (the same scale as that in Figure 4) recorded in the test by the FBG sensor at *Re* = 15200 and *a* = 80°, along with the velocity signal *u*. Evidently, the $q_s$ signal is largely due to the structural vibration and background noise. Its amplitude is greatly reduced, compared with that at the same *Re* and *a* when the cylinder was heated (Figure 4b). In fact, the maximum ratio of $q_{s,rms}$ with the cylinder heated to that without heating is about 6 (near *a* = 80°), while the minimum is about 2. This is a good indication of the signal-to-noise ratio range. Furthermore, the corresponding $E_{q_S}$ (not shown) does not show any peak at $f_s^* \approx 0.2$. These results point to a negligible effect of the structural vibration on the present temperature measurement.

**5.2 Closely Correlated $q_s$ and *u***

The spectral coherence $Coh_{q_s u}$ [$\equiv (Co_{q_s u}^2 + Q_{q_s u}^2)/E_{q_s}E_u$, where $Co_{q_s u}$ and $Q_{q_s u}$ are the cospectrum and quadrature spectrum of $q_s$ and *u*, respectively] provides a measure of the degree of correlation between the

Fourier components of $q_s$ and *u*. $Coh_{q_s u}$ (Figure 7) between $q_s$ (*a* = 80°) and *u* reaches 0.9 at $f_s^* \approx 0.2$, indicating a high level of correlation. This observation is consistent with the fact that the fluctuating temperature on the cylinder surface is closely linked to the vortex formation and shedding. The highly correlated $q_s$ and *u* lends further credence to the present measurement technique.

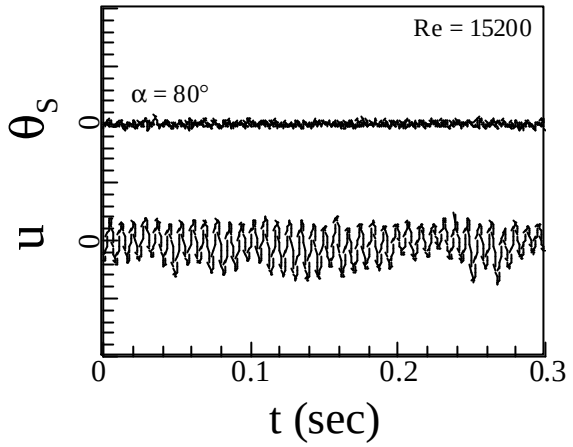


*Figure 6. Time histories of the streamwise fluctuating velocity u (the hot wire was located at x/d = 2 and y/d = 1.5) and $q_s$ at Re = 15200 and a = 80°. The cylinder was unheated.*

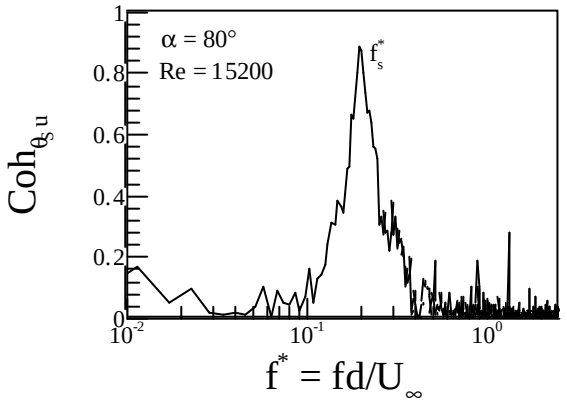


*Figure 7. Spectral coherences $Coh_{q_s u}$ between the fluctuating surface temperature $q_s$ and the streamwise fluctuating velocity u at a = 80° and Re = 15200. The hot wire was located at x/d = 2 and y/d = 1.5.*

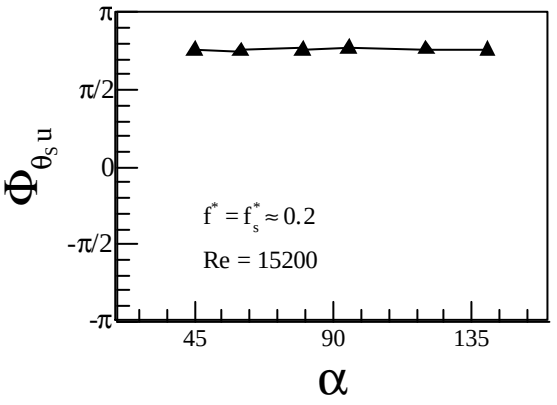


*Figure 8. Spectral phase angle $\Phi_{q_s u}$ at various a between the fluctuating surface temperature $q_s$ and the streamwise fluctuating velocity u (Re = 15200). The hot wire was located at x/d = 2 and y/d = 1.5.*

The spectral phase shift $\Phi_{q_s u}(\equiv \tan^{-1} Q_{q_s u} / Co_{q_s u})$ between $q_s$ and $u$ at $f_s^*$ (Figure 8) tends to be anti-phased, approaching $\pi$, irrespective of the $a$ value ($Re$ = 15200). The corresponding $Co_{q_s u}$ exhibits a negative extremum at $f_s^*$, as illustrated in Figure 9. The location of the hot wire was unchanged throughout the experiments. The observation is reasonable. When the boundary layer separates from the cylinder surface, the streamwise velocity measured by the hot-wire at $x/d$ = 2 and $y/d$ = 1.5 should be increased, giving rise to a positive $u$. Meanwhile, heat is removed from the cylinder surface, resulting in a negative $q_s$.

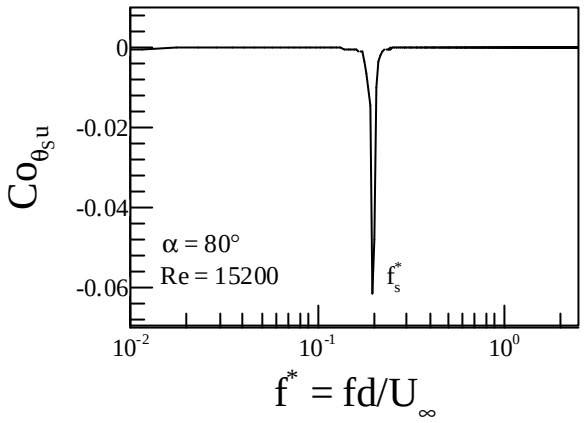


*Figure 9. Co-spectrum $Co_{q_s u}$ between the fluctuating surface temperature $q_s$ and the streamwise fluctuating velocity u at a = 80° and Re = 15200. The hot wire was located at x/d = 2 and y/d = 1.5.*

**5.3 Probability Density Function**

The probability density function (PDF), $P_{q_s}$, of $q_s$ (Figure 10) at $a$ = 80° ($Re$ = 15200) is quite symmetrical about $q_s / q_{s,rms} = 0$ and appears to follow the normal distribution. The maximum magnitude of $q_s$ approximately triples $q_{s,rms}$. This observation is essentially in consistence with Boulos and Pei (1974)'s investigation on the heat transfer from a circular cylinder in a turbulent air flow at $Re$ = 3000 ~ 9000. Their results indicated that the PDF of the measured heat transfer rate is normal around the flow separation point (e.g. at $a$ = 80° ~ 90°) under both constant wall temperature (CTW) and constant heat flux (CHF) conditions.

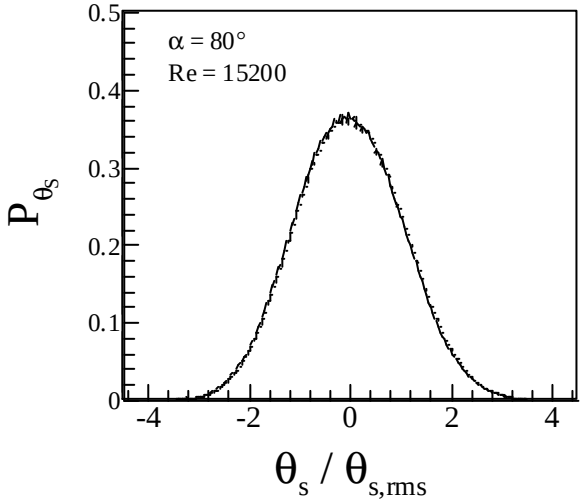


*Figure 10. The probability density function $P_{q_s}$ of the fluctuating surface temperature $q_s$ measured using the FBG sensor. Re = 15200, a = 80°.*

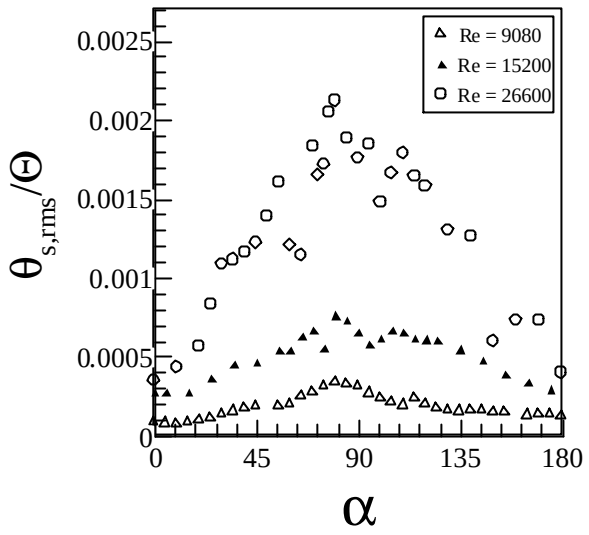


*Figure 11. Circumferential distribution of the rms value $q_{s,rms}/\Theta$ of the fluctuating surface temperature $q_s$. ? , Re = 9080; ? , Re = 15200; ?, Re = 26600.*

**5.4 Circumferential Distribution of $q_{s,rms}$**

The circumferential distribution of $q_{s,rms}$ for *Re* = 9,080, 15,200 and 26,600 is given in Figure 11. The $q_{s,rms}/\Theta$ value displays a maximum near $a \approx 80°$ for the present range of *Re* (Figure 11). This location is coincident with the minimum static temperature (Figure 3). Both observations may be attributed to the turbulent eddy motion after flow separation. On the other hand, the minimum $q_{s,rms}/\Theta$ occurs at the leading and trailing stagnation points. The present observation conforms to Scholten and Murray (1998)'s heat flux measurement, which indicated a great fluctuation in the heat flux on the cylinder surface at $a = 85°$, compared with that at $a = 0°$ (Re = 21580).

The maximum value of $q_{s,rms}/\Theta$ (Figure 12) increases for larger *Re*. Krall and Eckert (1973) proposed that the boundary layer around a circular cylinder subjected to a uniform cross-flow became rapidly thinner as *Re* increases. This implies that the cylinder surface temperature is more prone to the vortex formation and shedding perturbation, fluctuating more with increasing *Re* (Figures 11 and 12), especially near the flow separation region.

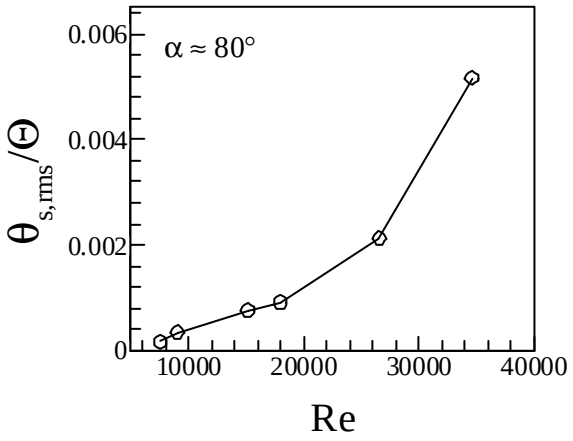


*Figure 12. Influence of Re on the maximum rms value, $q_{s,rms}/\Theta$, of the fluctuating surface temperature $q_s$ near a » 80°.*

## 6. CONCLUSIONS

Attempt has been made to use the fiber-optic Bragg grating (FBG) sensor to measure simultaneously static and fluctuating surface temperatures on a heated circular cylinder in a cross-flow. The investigation leads to the following conclusions:

1. The local static surface temperature $\overline{q_s}/\Theta$ measured using the FBG sensor is in good agreement with that simultaneously obtained by a *K*-type thermocouple. Furthermore, the circumferential distribution of $\overline{q_s}/\Theta$ is qualitatively consistent with the reported *Nu* data. At *Re* = 7600, for example, a maximum $\overline{q_s}/\Theta$ occurs at $a \approx 60°$, corresponding to the minimum heat transfer coefficient *Nu* and probably to the flow separation point. As $a$ increases from 60° to 80°, $\overline{q_s}/\Theta$ drops rapidly, reaching the minimum at $a \approx 80°$; accordingly, there is a quick climb in *Nu*. The observation is probably due to the turbulent eddy motion after flow separation, which is supported by a prominent peak in the rms value $q_{s,rms}$ of $q_s$ near $a \approx 80°$. For further increase in $a$, $\overline{q_s}/\Theta$ increases due to a decrease in *Nu*. The results suggest that the FBG sensor may provide reliable measurements for the static temperature on the cylinder surface.
2. The dynamic response of the FBG sensor is excellent. The fluctuating temperature $q_s/\Theta$ is closely correlated to the hot-wire measurement. The power spectrum $E_{q_s}$ exhibits a prominent peak at the vortex shedding frequency $f_s^* \approx 0.2$, as identified in $E_u$. The $q_s$- and *u*-signals tend to be anti-phased at $f_s^*$, their spectral coherence reaching 0.9. These results indicate that the FBG sensor is adequate in resolving the fluctuating surface temperature of a cylinder in a cross-flow.

In view of the uniqueness in many aspects and being at an affordable cost, it is expected that the FBG sensor may have an excellent prospect in the measurements of bath static and fluctuating temperatures.

**ACKNOWLEDGEMENTS**

The authors wish to acknowledge support by the Central Research Grant of The Hong Kong Polytechnic University through Grants G-T408, G-YD21 and G-T444.

## REFERENCES

Achenbach, E. 1968 Distribution of local pressure and skin friction around a circular cylinder in cross-flow up to Re = 5 x $10^6$. *Journal of Fluid Mechanics* **34**(4), 625-639.

Boulos, M. I. and Pei, D. C. T. 1973 Heat and mass transfer from cylinders to a turbulent fluid stream-A critical review. *The Canadian Journal of Chemical Engineering* **51**(12), 673-679.

Boulos, M. I. and Pei, D. C. T. 1974 Dynamics of heat transfer from cylinders in a turbulent air stream. *International Journal of Heat and Mass Transfer* **17**, 767-783.

Chen, S. S. 1987 *Flow-induced vibration of circular cylindrical structures*. Hemisphere Publishing Corporation, Washington.

Dwyer, H. A. and Mccroskey, W. J. 1973 Oscillating flow over a cylinder at large Reynolds number. *Journal of Fluid Mechanics* **61**(4), 753-767.

Giedt, W. H. 1949 Investigation of variation of point unit heat-transfer coefficient around a cylinder normal to an air stream. *Transactions of the ASME*, May, 375-381.

Goldstein, S. 1965 *Modern Developments in Fluid Mechanics: an account of theory and experiment relating to boundary layers, turbulent motion and wakes*. Dover Publications, Inc. New York.

Gottlieb, M. and Brandt, G. B. 1979 Measurement of temperature with optical fibers. *Fibre Optic Conference*, Chicago, pp. 236 – 242.

Grattan, K. T. V. 1987 The use of fibre optic techniques for temperature measurement. *Measurement and Control* **20**(6), 32 – 39.

Higuchi, H., Kim, H. J. and Farell, C. 1989 On flow separation and reattachment around a circular cylinder at critical Reynolds numbers. *Journal of Fluid Mechanics* **200**, 149-171.

Hill, K. O., Fujii, Y., Johnson, D. C. and Kawasaki, B. S. 1978 Photosensitivity in optical fiber waveguides: Application to reflection filter fabrication. *Applied Physics Letters* **32**(10), 647-649.

Ho, H. L., Jin, W., Chan, C. C., Zhou, Y. and Wang, X. W. 2002 A fiber Bragg grating sensor for static and dynamic measurands. *Sensors and Actuators A* **96**, 21 – 24.

Holman, J. P. 1997 *Heat Transfer, 8$^{th}$ ed*. Mcgraw-Hill Companies, New York. pp. 248 – 255, 303.

Jin, W., Zhou, Y., Chan, P. K. C. and Xu, H. G. 2000 A fibre-optic grating sensor for the study of flow-induced vibrations. *Sensors and Actuators* **79**, 36-45.

Kersey, A. D., Davis, M. A., Patrick, H. J., LeBlanc, M., Koo, K. P., Askins, C. G., Putnam, M. A. and Friebele, E. J. 1997 Fiber grating sensors. *Journal of Lightwave Technology* **15**, 1442-1462.

King, R. 1977 A review of vortex shedding research and its application. *Ocean Engineering* **4**, 141-171.

Krall, K. M. and Eckert, E. R. G. 1973 Local heat transfer around a cylinder at low Reynolds number. *Journal of Heat Transfer* **95**, 273 – 275.

Marton, L. and Marton, C. 1981 *Methods of Experimental Physics: Volume 18, Fluid Dynamics, Part B*. Academic Press, Inc. (London) LTD.

Michalski, L., Eckersdorf, K. and McGhee, J. 1991 *Temperature Measurement*. John Wiley & Sons Ltd. Baffins Lane, Chichester, West Sussex PO19 1UD, England.

Morey, W. W., Meltz, G. and Glenn, W. H. 1989 Bragg-grating temperature and strain sensors. *The Sixth Optical Fibre Sensor Conference*, Paris, Springer Proc. **44**, 526-531.

Morris, A. S. 1993 *Principles of measurement and instrumentation*. Second edition. Redwood Books Ltd, Trowbridge, Wiltshire, Great Britain.

Morrison, R. 1984 *Instrumentation Fundamentals and Applications*. John Wiley & Sons, New York.

Perking Jr, H. C. and Leppert, G. 1964 Local heat-transfer coefficients on a uniformly heated cylinder. *International Journal of Heat and mass Transfer* **7**, 143-158.

Sandberg, C. and Haile, L. 1987 Fiber optic application in pipes and pipelines. *IEEE Transactions on Industry Applications IA-23*(6), 1061.

Schlichting, H. 1979. *Boundary-Layer Theory*, New York, McGraw-Hill.

Scholten, J. W. and Murray, D. B. 1998 Unsteady heat transfer and velocity of a cylinder in cross flow: part 1, Low freestream turbulence. *International Journal of Heat and Mass Transfer* **41**(10), 1139-1148.

Valvano, J. W. 1992 Temperature measurements. *Advances in Heat Transfer* **22**, 359-436.

Zhou, Y., So, R. M. C., Jin, W., Xu, H. G. and Chan, P. K. C. 1999 Dynamic strain measurements of a circular cylinder in a cross flow using a fibre Bragg grating sensor. *Experiments in Fluid* **27**, 359-367.

Zhou, Y., Wang, Z. J., So, R. M. C., Xu, S. J. and Jin, W. 2001 Free vibrations of two side-by-side cylinders in a cross flow. *Journal of Fluid Mechanics* **443**, 197 – 229.

Zukauskas, A. and Ziugzda, J. 1985 *Heat Transfer of a Cylinder in Crossflow;* translated by E. Bagdonaite ; edited by G. F. Hewitt. Hemisphere Pub., Washington.